The formation process of a paleoindian open-air site in Central Brazil: integrating lithic analysis, radiocarbon and luminescence dating

Lucas Bueno [a], James Feathers [b,*], Paulo De Blasis [c]

[a] Laboratório de Estudos Interdisciplinares em Arquelogia, Universidade Federal de Santa Catarina, Florianópolis, Santa Catarina, Brazil
[b] Department of Anthropology, University of Washington, Seattle, WA 98195-3100, United States
[c] Museu de Arqueologia e Etnologia, Universidade de São Paulo, São Paulo, Brazil

A B S T R A C T

Lithic analysis, radiocarbon dating and luminescence dating are applied to a stratified open-air Paleo-indian site in Central Brazil, lending some balance to a published record dominated by rock shelter sites. Most lithics are found in two discrete occupation layers. Lithics found outside these layers are attributed to post-depositional movement of small flakes mainly upwards. Single-grain luminescence dating on quartz grains also suggest post-depositional movement. Both wind and bioturbation are suspected mechanisms. The luminescence analysis does not provide precise depositional dates in this situation but does support such dates suggested by radiocarbon.

© 2012 Elsevier Ltd. All rights reserved.

1. Introduction

Central Brazil has a rich Paleoindian record but most studied sites dating to the Pleistocene/Holocene transition are found in rockshelters (Kipnis, 1998; Prous and Fogaça, 1999; Schmitz, 1987). Only in sheltered sites has the Paleoindian record been well-dated, and also only in these sites has the transition between Paleoindian and subsequent technologies been described. Little is known about open-air occupations, although presumably they are important for understanding Paleoindian settlement and subsistence patterns. Schmitz (1980), for example, has suggested that populations aggregated in rockshelters during summer rainy seasons but dispersed to open-air locations along small rivers and creeks during dry seasons. Lack of detailed studies of open-air sites has prevented testing this hypothesis as well as a better understanding of Paleo-indian territoriality. Although hundreds of open-air sites have been recorded, they rarely allow for clear stratigraphic sequences or good conditions for dating (Bueno, 2008; Kipnis, 1998; Prous and Fogaça, 1999; Rodet, 2006).

This paper provides a detailed analysis of the chronology and lithic technology of an extensively excavated Paleoindian open-air site near the city of Miracema do Tocantins, located in a paleo-dune field above the Tocantins River, at the northern outskirts of the Central Brazilian Plateau. Particular attention is paid to site formation processes in dune environments and the extent to which post-depositional sand movements and mixing might have affected the understanding of the occupation sequence and the detected changes in lithic technology.

2. Archaeological background: open-air sites and the early occupation of Central Brazilian Plateau

The Central Brazilian Plateau (CBP) is an uplifted region bordered by lowlands to the north (Amazonia), west/southwest (Chaco lowlands) and east (Atlantic seaboard) (Fig. 1). The main geologic features are flat, dry Mesozoic-aged sandstone plateaus, or *chapadas*, occasionally interrupted by pre-Cambrian mountain ranges (*serras*). Altitudes range from 200 to about 1000 m. A more rugged topography consisting of older limestone and quartzite mountains is found in the southeastern portion. Several large rivers, such as the Tocantins and the São Francisco, provide drainage, mostly to the north. Savannah-like *cerrado* vegetation

* Corresponding author.
  E-mail address: jimf@u.washington.edu (J. Feathers).
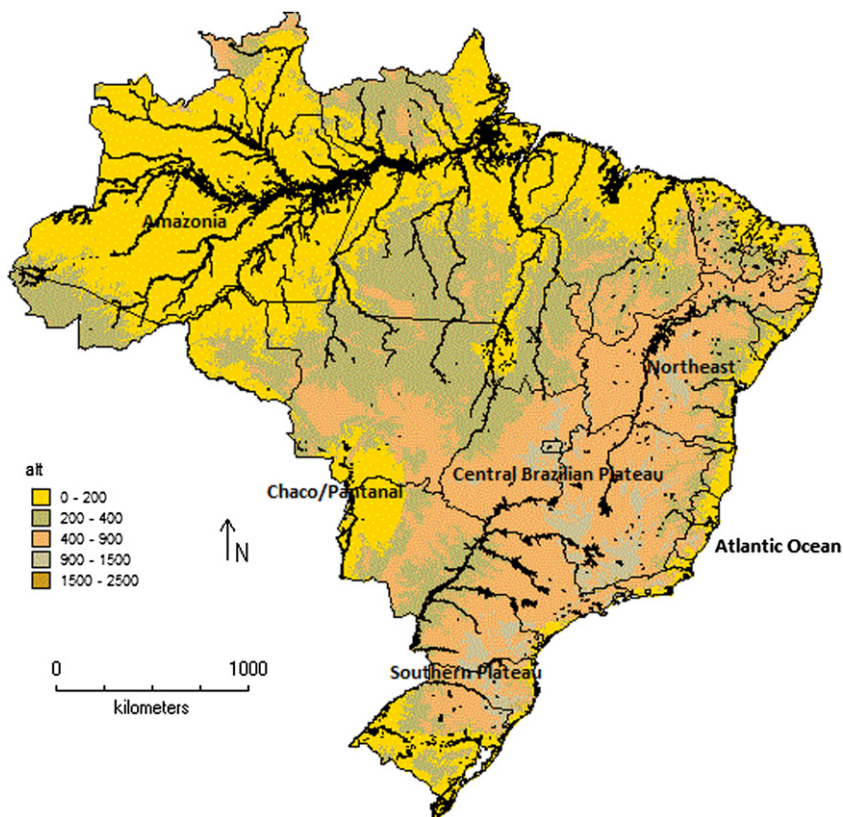
Fig. 1. Relief map of Brazil (contours in meters above mean sea level) showing the Central Brazilian Plateau and major river drainages. The *X* near the center of the country gives the location of Miracema do Tocantins.

dominates the landscape, though denser forests are found along rivers and canyons and on the moister slopes of the *serras* (Ab'Saber 1982, Ledru 1993, Oliveira and Marquis, 2002).

Hundreds of rockshelters are found along the steep slopes, or *cuestas*, of the *chapadas*, usually along small tributaries to the larger rivers. They are also found in limestone formations in the southeastern portion of the plateau (Araujo and Neves, 2010; Prous et al., 1998; Prous and Rodet, 2009). Paleoindian archaeological remains in the shelters date as early as 14–13.5 ka cal BP, but most sites date between 12.8 and 9.5 ka cal BP (Bueno, 2011; Dias, 2004; Prous and Fogaça, 1999; Kipnis, 1998; Oliveira and Viana, 1999/2000). Lithics are commonly characterized by formal, well-finished unifacial artifacts. The most distinctive are *limaces*, which are large, elongated flakes retouched into cutting/scraping tools with flat-convex transversal sections (Fig. 2). Expedient unifacial tools are also common. These assemblages are commonly referred to as Itaparica Tradition and, although they are defined mainly by these intensely retouched and curated unifacial tools, a few finely retouched stemmed bifacial points, and bifacially retouched flakes, are also found in most of these assemblages (Bueno, 2007a; Schmitz, 1987; Fogaça, 2001; Lourdeau, 2010).

Itaparica sites in the CBP sometimes form site aggregates such as in the Serranópolis, Peruaçu, Serra da Capivara and Lajeado/Miracema (middle Tocantins) areas (Schmitz et al., 2004; Fogaça, 2001; Rodet, 2006; Guidon, 1986; Bueno, 2007a). Whether these aggregates reflect settlement patterns of cyclic and recurrent occupations or are a matter of sample bias, is still an open question. What is indisputable is that late Pleistocene/early Holocene sites with similar formal and quantitative lithic characteristics are found over distances of more than 2000 km (Schmitz, 1981; Lourdeau, 2010; Bueno, 2011). These similarities are based on assemblage composition, raw material procurement

Fig. 2. Silicified sand stone limaces of the Itaparica Tradition from Lajeado region. Increments are in cm.

Fig. 3. General photo of the site showing dune from a distance.

behavior, and production process of formal artifacts, particularly the limace. There are also similarities in site location decisions and in local inter-site assemblage variability (Bueno, 2005/2006: p. 15). In the middle Tocantins, Peruaçu and Serranópolis regions there is also evidence of inter-regional variation in the *chaine operatoire* related to production of formal artifact types that may relate to cultural transmission mechanisms and histories (Bueno, 2005/2006, 2007b, Lourdeau, 2010). Subsistence patterns are also similar, with evidence of intensive exploitation of broad-spectrum resources based on medium- and small-size game and on intensive foraging for wild fruits and edible roots (Kipnis, 2003; Rosa, 2004).

The site of Miracema do Tocantins is located upon Pleistocene dune formations along the western margin of the Tocantins River, which flows north to Amazonia (Fig. 3). Several sites in these dunes were identified in the late 1990s during a CRM project when they were exposed during highway construction. The sites, buried more than 2 m deep, have been radiocarbon dated to the Pleistocene/Holocene transition. The dunes are currently stable with large flat tops covered by *cerrado* bushes. They provide ready access to the river plus broad vantage to the Serra do Lajeado to the southeast and to the transitional Amazonian vegetation to the north.

Dozens of lithic sites, typologically dating to the Paleoindian and Archaic periods, are found in the rolling hills between the eastern margin of the river and the serra escarpment (Bueno, 2007a). These sites are located on erosional surfaces and have no sub-surface remains. Several of them contain thousands of artifacts representing the entire lithic reduction process, but as palimpsests of several occupations, the sequence of technological change is difficult to disentangle. No organics are preserved for radiocarbon dating. Thus, a buried stratified site like Miracema do Tocantins, with opportunities for both radiocarbon and luminescence dating, has considerable value for understanding the early prehistory of this region.

Excavations have occurred at only five of the many sites recorded along these dunes. Miracema do Tocantins has received the most attention, with an excavated area of 68 m^2 from within a 500 × 200 m tract where most artifacts have been found. The excavation included both 52 m^2 of trenches and five blocks of horizontal exposure in the areas of highest artifact density (Fig. 4). A total of 10,873 lithic artifacts have been recovered, 60% of them from eight excavation units in the center of the site. Lithics appear in discrete concentrations, often with refitting possible within a concentration. The 2 × 2 m excavation units were dug in 10 cm arbitrary levels (Bueno, 2007a).

Deposits consist of fairly homogeneous sand. The top 30 cm consists of a dark brown organic soil horizon. Similar organic layers are found in some places as deep as 90 cm, suggesting ancient vegetated surfaces. Below the surface organic horizon is beige to brown sand, extending to 2.5 m and containing most of the archaeological remains. This sand grades into a yellow/orange sand that extends to the base of the excavation at 3.5 m. These dunes can occasionally reach a depth of 40 m, but excavation beyond 3.5 m was not safe due to unstable walls. Archaeological materials are rarely found below 3 m (Figs. 5 and 6). Roots extend as deep as 1.5 m.

Archaeological remains, mostly chipped lithics, fire-cracked rock and charcoal, are concentrated into two horizontal layers in the beige/brown sand, one at 90–120 cm and one at 170–220 cm.[1] Scattered small lithic flakes (<1 cm) and charcoal are found outside these horizons. Charcoal was systematically collected from screening of 10 cm excavation layers, but two samples (Beta 148339 and Gif 11833) were collected *in situ*. Charcoal was wrapped in

---

[1] An upper ceramic-bearing horizon has been detected at other sites, but is barely visible here, although a calibrated radiocarbon date of 1080–1290 BP, Gif 11833, was obtained at 60 cm, which is within the accepted range of ceramics in this region.
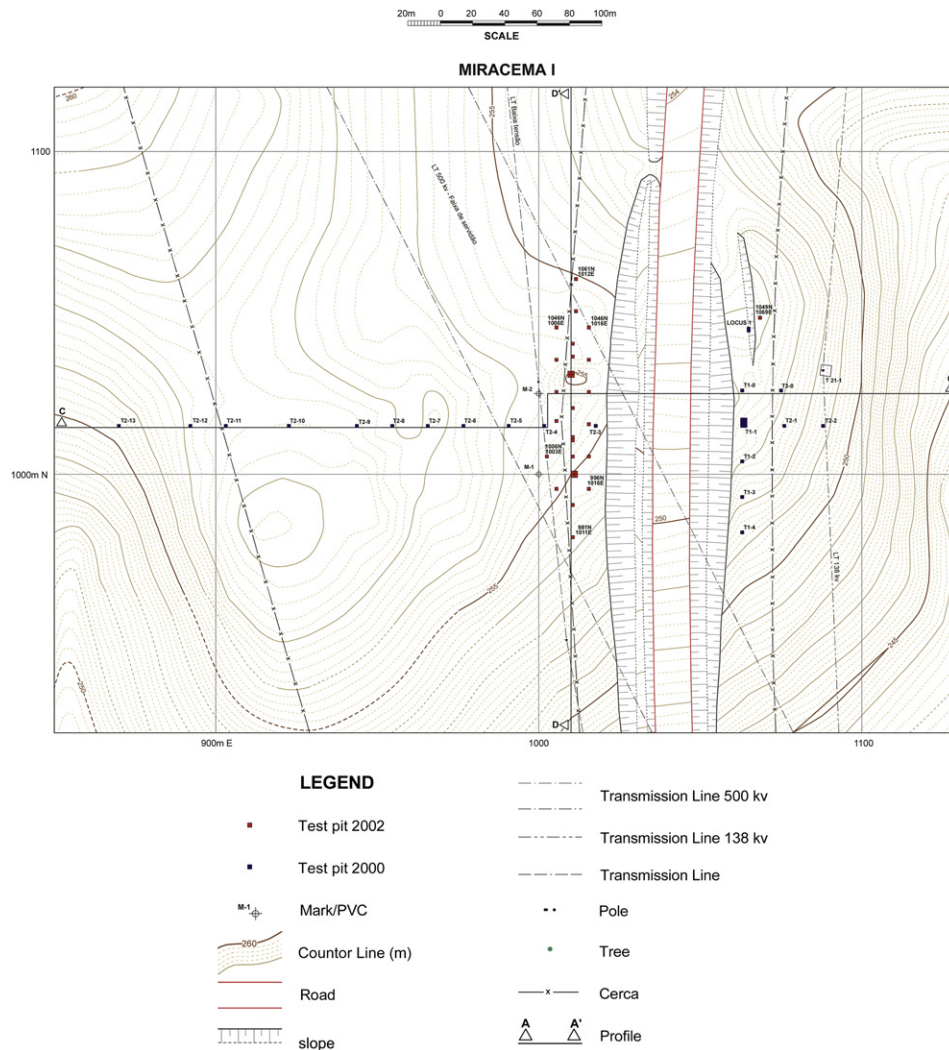
Fig. 4. Topographic map of the Miracema do Tocantins site, showing test units on either side of the road cut.

aluminum foil and stored in plastic bags, all of the same size. The number of bags amounts to a proxy for the overall amount of charcoal collected from each layer.

The lithics from the two horizons differ markedly. The lower horizon is characterized by finished unifacial tools, abundant flakes from unifacial or bifacial reduction sequences, and small retouch flakes (defined as <1 cm). Raw material is mainly fine-grained sandstone and quartzite, with occasional good quality silex and quartz. No structural features have been found at this level.

The upper level assemblage is composed mainly of burned pebbles, with a few quartz and quartzite flakes and some formal tools. The only bifacial projectile point — a triangular, unstemmed variant made on quartz — was also found in this upper horizon. Also noteworthy is the presence of intact fire-cracked rock/charcoal features ("hearths") in the upper level. Artifacts and charcoal in the lower layer were more dispersed. Stratigraphic sequences with similar variability in composition and technology are found at other nearby excavated dune sites.

Table 1 gives amounts of lithics and charcoal for each 10-cm level from the central excavated area (17 2 × 2 m units). Both have a continuous stratigraphic distribution with identifiable peaks at levels 90–120 cm (upper horizon) and levels 190–220 cm (lower horizon). The question posed is whether this represents continuous

occupation or two discrete occupation periods blurred by post-depositional mixing? Bioturbation, often intense in the tropics, did not visually appear prominent in this sandy micro-environment; although it could account for the vertical displacement of the artifacts (Ahlbrandt et al., 1978). The presence of recognizable features in the upper horizon suggests this is not the case (Leigh, 2001), but as will be considered later, the presence of structure and the lack of any visible evidence may not preclude the possibility of extensive bioturbation.

3. Radiocarbon dating

The radiocarbon dates point to three pulses of dune occupation (Table 2). The most recent (Gif 11833) refers to a ceramic horizon detected across the dunes area and beyond, and will not be considered here. All other dates were obtained from the excavations in the central area of the site, with the exception of one (Beta 148338) drawn from Locus 2 excavations on a lower flank. These dates are bimodal with one group clustering between 5950 and 6890 cal BP and the other between 10,270 and 12,400 cal BP. The absence of intermediate dates reinforces the perception of two discrete occupations. Can the lithic scatter between the clustered levels be explained then by post-depositional movement? We

Fig. 5. Test unit N1026E1006 showing the stratigraphy of profile west. Total depth is 260 cm.

Table 1
Number of lithic debris and charcoal bags per 10 cm level (summed across 17 2 × 2 m excavation units).

Level (in cm)	Lithics	Charcoal	Level (in cm)	Lithics	Charcoal
0–10	–	–	150–160	190	4
10–20	2	–	160–170	342	3
20–30	9	–	170–180	537	4
30–40	10	–	180–190	404	3
40–50	25	–	190–200	1326	4
50–60	25	–	200–210	865	6
60–70	42	–	210 = −220	788	5
70–80	70	–	220–230	133	2
80–90	109	2	230–240	60	2
90–100	134	5	240–250	33	1
100–110	134	6	250–260	12	1
110–120	133	3	260–270	8	1
120–130	103	–	270–280	6	–
130–140	113	–	280–290	9	–
140–150	118	2	3290–300	6	–

Table 2
[14]C dates for Miracema do Tocantins site ($N = 10$). Two sigma calibrations performed with CALIB 6.0 (Stuiver and Reimer, 1993) using curve SHCAL04 (McCormac et al., 2004).

Location	Depth (cm)	Standard date	Cal BP	Lab ID
N1036/E1006	50–60	1326 ± 50	1080–1290	Gif 11833
N1001/E1012	90–100	5411 ± 65	5950–6290	Gif 11834
N1001/E1011	100–110	5980 ± 50	6640–6890	Beta 190079
N991/E1011	150–160	9397 ± 80	10,270–10,750	Gif 11835
N1001/E1012	160–170	10,520 ± 90	12,070–12,400	Beta 190080
T1B1	160–170	9790 ± 70	10,790–11,270	Beta 148339
N1036/E1006	170–180	9650 ± 60	10,730–11,170	Beta 190081
N1032/E1011	210–220	9456 ± 95	10,300–11,070	Gif 11836
N1037/E1011	230–240	9990 ± 60	11,220–11,690	Beta 168605
Locus 2	60–70	5650 ± 70	6220–6550	Beta 148338

evaluate this question with single-grain optically stimulated luminescence (OSL)[2] and with in-depth lithic analysis.

4. Luminescence dating

While the vertical distribution of radiocarbon ages can give some confidence of stratigraphic integrity, radiocarbon addresses the age of the carbon, not the age of the deposit. (The radiocarbon ages could be out of order without any post-depositional mixing.) An advantage of OSL dating is the potential to directly assess sediment mixing, whether the grains themselves have moved. This is possible by computing the equivalent dose (D_e) of single grains, the distribution of which can be related to sediment mixing if other sources of variation are ruled out. A luminescence age is the quotient of equivalent dose, a measure of the absorbed dose accumulated through time, divided by the dose rate. We have performed single-grain dating on five samples collected in 2002. Table 3 gives the provenience information for each sample. Notice that UW825, UW826 and UW827 are from the same unit.

4.1. Procedures

Procedures are similar to those followed at Lapa Vermelha in the southeastern part of the CBP (Feathers et al., 2010). Samples were collected in light-tight containers and removed in the laboratory under red light conditions for preparation. Quartz was isolated by

Fig. 6. Test unit N1001E1002 showing the lithic assemblage from level 10 and the stratigraphy of profile north. Total depth is 110 cm.

---

[2] In this text both C14 and OSL dating are examined. While "present", for calibrated radiocarbon dates, refers to the year of 1950, for OSL dates the reference is 2010. Although a correction value of sixty years could be applied, we decided to keep it as it is, given the low impact this difference has on Paleoindian chronology.

Table 3
Provenience information for each OSL collected sample.

Lab number	Sample #	Test unit	Depth (cm)	Location
UW823	OSL 1	N1606 E1063 west wall	161	Lower lithic horizon
UW824	OSL 2	N1026 E1006 east wall	204	Lower lithic horizon
UW825	OSL 3	N1037 E1011 east wall	261	Lower lithic horizon
UW826	OSL 4	N1037 E1011 east wall	175	Between two lithic horizons
UW827	OSL 5	N1037 E1011 east wall	84	Above upper lithic horizon

Table 4
Concentrations of the major radionuclides and beta dose rates.

Sample	^{238}U (ppm)	^{232}Th (ppm)	K (%)	Beta dose rate (Gy/ka)	
				α-counting/flame photometry	ß-counting
UW823	0.65 ± 0.07	2.43 ± 0.59	0.02 ± 0.01	0.18 ± 0.02	0.21 ± 0.02
UW824	0.25 ± 0.05	2.37 ± 0.53	0.04 ± 0.01	0.14 ± 0.02	0.19 ± 0.02
UW825	0.53 ± 0.07	2.25 ± 0.57	0.05 ± 0.01	0.18 ± 0.02	0.20 ± 0.02
UW826	0.16 ± 0.07	3.02 ± 0.66	0.04 ± 0.01	0.14 ± 0.02	0.19 ± 0.02
UW827	0.38 ± 0.05	1.88 ± 0.35	0.04 ± 0.01	0.14 ± 0.03	0.18 ± 0.01
Modern soil sample	0.37 ± 0.05	0.90 ± 0.35	0.04 ± 0.01		

sieving, treatment with HCl and H_2O_2, etching for 40 min in 48% HF, and density separating using sodium polytungstate solution at 2.67 specific gravity. D_e was measured on two different grain-size fractions, 125–150 μm and 180–212 μm, but the ages reported here are based only on the larger size-fraction. The smaller size compromises single grain resolution to some degree because of the possibility of more than one grain fitting into the 300 μm diameter holes on the measuring disks. The smaller size was used on the expectation that the quartz would not be highly sensitive and that the probability of more than one grain in a hole providing a signal would be low. D_e was measured using the single-aliquot regeneration (SAR) protocol (Murray and Wintle, 2000) on a Risø TL-DA-15 reader equipped with a single-grain attachment containing a 532 nm laser for stimulation. The laser was set at 90% full power (50 mW/cm). Detection was through 7.5 mm of U340 ultraviolet filters. Exposures were for 0.8 s with the first 0.06 s used for analysis and the last 0.65–0.8 s for background. Preheats of 240 °C for 10 s after the natural and each regeneration dose and of 200 °C for 1 s after each test dose were employed. Other preheat combinations were not attempted, because this combination has proven satisfactory for other work done in Central Brazil (Feathers et al., 2010; Araujo et al., 2008). Test doses were about 3 Gy. The SAR protocol employs only one aliquot (one grain in this case) and applies a series of regeneration doses to calibrate the natural signal in terms of D_e. A series of identical test doses are used after each regeneration signal and the natural signal to correct for any sensitivity changes during the measurement sequence.

One advantage of doing single-grain dating is the opportunity to select only those grains whose luminescence properties conform to a set of quality standards. Grains were rejected for analysis if (1) the signal was small (the signal on the test dose less than three times the standard deviation of the background), (2) the ratio of sensitivity-corrected signals from two identical regeneration doses applied at the beginning and end of the SAR sequence was not between 0.8 and 1.2, (3) the sensitivity corrected signal on a zero dose was more than 10% of the natural signal, (4) the corrected natural signal did not intersect the growth curve created by the regeneration doses, and (5) application of an infrared exposure after two regeneration doses caused the sensitivity corrected signals to lie beyond one-sigma error of the curve created by the other regeneration doses (indicative of feldspar contamination). D_e distributions among grains were evaluated using central age and minimum age models (Galbraith et al., 1999) and the finite mixture model (Roberts et al., 2000).

Dose rate was measured in the laboratory using thick source alpha counting, flame photometry and beta counting. $CaSO_4$ dosimeters were left at the sample locations but these were never retrieved. The laboratory measurements are probably sufficient, however, because the variation in radioactivity among the samples, some of which are several meters apart, is small. The dose rate is low for these samples, and consequently the cosmic dose rate forms

a significant portion of the total dose rate. The cosmic dose rate was calculated following Prescott and Hutton (1988) assuming sediment density of 1.5 g/cm³ and that current depths have prevailed through most of the depositional time. The ages were also recalculated using half the current depth, which would assume a rather constant sedimentation through time.

4.2. Dose rate

The concentrations of the major radionuclides are given in Table 4, which also includes the beta dose rate calculated in two ways. The beta dose rate derived directly from beta counting is systematically higher than that calculated from alpha counting (assuming secular equilibrium) and flame photometry. The discrepancy, significant for three of the samples, may reflect some disequilibrium in the uranium decay chain. If fractionation between the parent ^{238}U and daughter ^{234}U has occurred, with the daughter becoming depleted, the higher dose rate from beta counting could be due to the strong beta emission from ^{234}Pa, an intermediate daughter nearly always in equilibrium with ^{238}U. Because such fractionation is usually due to the solubility of some forms of U in water, the fractionation likely occurred in the source deposit rather than in the dune. Whatever the cause of the discrepancy, beta counting, as a direct measure, is considered more accurate and was used for the beta dose rate in age calculation for all samples. Moisture content was taken to be 6 ± 4 percent (1σ), typical for sandy sediments (Brady, 1974) and encompassing current measured moisture (which ranged from 2 to 3 percent, but the samples were collected in the dry season). The difference in age due to differences in cosmic dose rate assuming different depositional modes (rapid versus prolonged) was not significant for any sample, but resulted in systematically lower ages assuming the prolonged mode, on the order of about 4%. This should not affect conclusions. Total dose rates are given in Table 5.

4.3. Equivalent dose

As a test of procedures, a dose recovery test was done on all samples from the 180–212 μm fraction. In this test, grains are first set to zero by exposure to the green laser for 1 s at 125 °C and then given a known dose. The SAR procedure is then applied to see if this

Table 5
Dose rates (Gy/ka), corrected for moisture content.

Sample	Alpha dose rate	Beta dose rate	Gamma dose rate	Cosmic dose rate	Total dose rate
UW823	0.004 ± 0.002	0.16 ± 0.02	0.18 ± 0.03	0.16 ± 0.03	0.50 ± 0.05
UW824	0.003 ± 0.002	0.13 ± 0.01	0.14 ± 0.02	0.15 ± 0.03	0.42 ± 0.04
UW825	0.003 ± 0.002	0.16 ± 0.02	0.17 ± 0.03	0.14 ± 0.03	0.47 ± 0.04
UW826	0.003 ± 0.002	0.15 ± 0.01	0.16 ± 0.03	0.16 ± 0.03	0.47 ± 0.05
UW827	0.003 ± 0.002	0.14 ± 0.01	0.13 ± 0.02	0.20 ± 0.04	0.47 ± 0.05

known dose can be obtained. The ratio of derived dose to administered dose ($n = 55$) was 1.01 ± 0.04 with an over-dispersion, (σ_b) of $17.9 \pm 0.3\%$. This magnitude of over-dispersion, a measure of spread that cannot be accounted for by differential precision, is the minimum that might be expected for a single-aged sample, due to variations in luminescence properties from grain to grain, machine scatter, or other variables intrinsic to the measurements or the grains. All extrinsic sources of σ_b — different depositional ages or differential dose rate — are controlled in dose recovery. Therefore σ_b values greater than about 15–20% in the D_e distributions of the natural samples can be attributed to these extrinsic factors.

Fig. 7 gives sample decay and growth curves. The sample distributions are summarized in Table 6. This gives the number of grains for which a D_e could be derived, the central tendency expressed as the central age model and σ_b. The σ_b is high for all samples, meaning that extrinsic factors must be taken into account. (Minimum age model D_e values will be discussed later.) To look at the structure of the data, a finite mixture model was applied. This model separates grains into single-aged components based on the input of a given σ_b value and the assumption of a log normal distribution of each component. The model estimates the number of components, the weighted average of each component (using the central age model), and the proportion of grains assigned to each component. The model provides two statistics for estimating the most likely number of components, maximum log likelihood and Bayes information criterion. An σ_b of 20%, slightly higher than that obtained in dose recovery, was used to account for intrinsic factors. The number of components derived is then a function of only extrinsic factors. Using 15% increased the number of components by one for three of the five samples, adding an older component in all three cases. Using 25% decreased the number of components by one for one of the five samples, eliminating a younger component.

Table 7 gives for each sample the D_e value for each component as well as the proportion of grains assigned to each component, using 20% over-dispersion.

About 1800 grains of the 180–212 μm fraction for each sample were measured, but only 5% had acceptable signals, most others being rejected because of weak signal not distinguishable from background. Such a low value prompted use of the 125–150 μm grains to provide effective single-grain resolution. But Table 6 shows the D_e for the smaller fraction is systematically higher. Inspection of finite mixture results shows that this difference is due to a larger number of high D_e values in the smaller fraction, probably due to grains with high natural signals which would be rejected in true single grain analysis because of recycle failures or failure to intersect the growth curve. In the 2–3 grain aliquots of the 125–150 μm fraction, some of these might get coupled with another grain with measurable signal, allowing the value to pass the rejection criteria. This suggests that even very small aliquots might not provide accurate D_e information (Feathers and Tunnicliffe, 2011).

Wind-blown sediments are often considered ideal for luminescence dating. The high over-dispersion indicated in Table 6 therefore requires some explanation. One possible reason is differential dose rate. The D_e is measured on single grains but the dose rate used to determine age is the bulk value from the entire sample. The dose rate, in particular the beta dose rate, may vary at the scale of single grains depending on the distribution of radioactive sources relative to the individual grains. For sandy sediments, one likely candidate for dose rate heterogeneity is ^{40}K from potassium feldspars, a strong beta emitter. A simulated model developed by Mayya et al. (2006) was applied to evaluate the potential, but could only explain a difference of 3–7% for the first two components, when they actually differ by 50–90%. Another
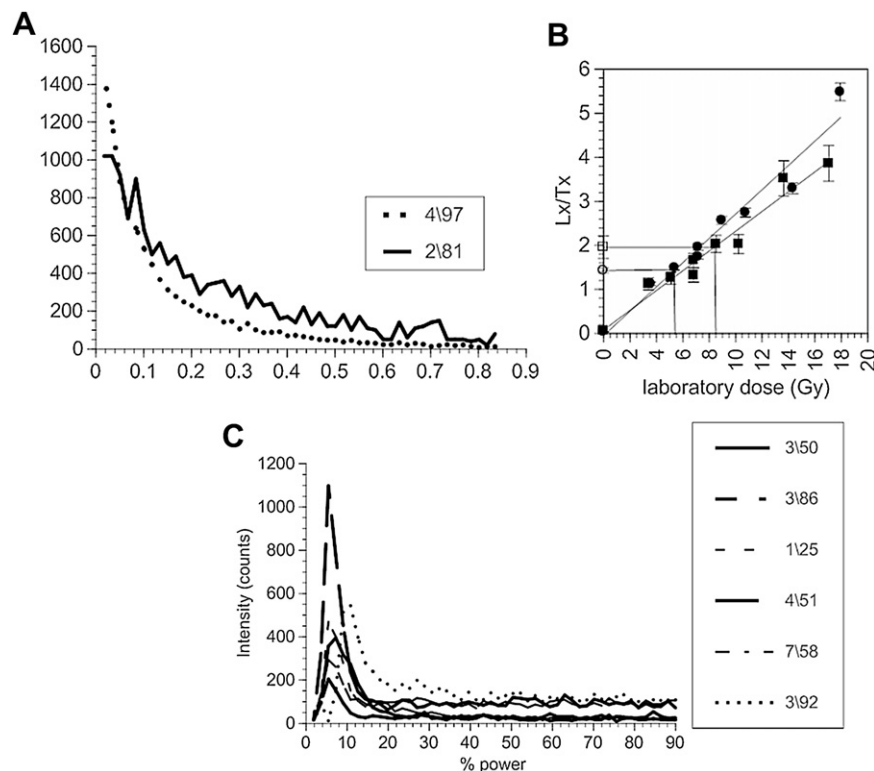
Fig. 7. A) Decay curves for two quartz grains (disk#/grain#) from UW825. The one from 2/81 has been multiplied by 10 to enhance visibility. B) Growth curves for the same samples shown in A, squares are 2/81 and circles are 4/97. Open symbols are the natural signals and lines are saturating exponential fits. Lx is the luminescence signal from the regeneration dose, and Tx is the signal from the test dose. C) LM-OSL curves from UW825 and UW826. Most grains appear dominated by the fast component as shown by the curves with the peak at less than 10% power, but a few, like 3\92, with a peak at greater than 10% power, appear dominated by the medium component.

Table 6
Natural distributions, central age and minimum age for 180–212 μm fraction except where indicated.

Sample	N	Central age D_e (Gy)	σ_b (%)	Central age D_e (Gy) for 125–150 μm	Minimum age D_e (Gy)
UW823	89	6.7 ± 0.3	39 ± 4	7.9 ± 0.3	4.3 ± 0.4
UW824	121	5.7 ± 0.2	38 ± 3	6.3 ± 0.2	3.8 ± 0.2
UW825	86	6.4 ± 0.4	50 ± 5	7.7 ± 0.4	3.6 ± 0.4
UW826	92	4.6 ± 0.2	44 ± 4	5.3 ± 0.2	2.8 ± 0.4
UW827	82	2.0 ± 0.2	66 ± 7	2.2 ± 0.2	0.9 ± 0.2

possible candidate for dose rate heterogeneity is pedogenic carbonates, which tend to be low in radioactivity, but these are not present in the deposits.

The other principle extrinsic cause for over-dispersion is different-aged grains, either because only some of the grains were fully bleached at time of deposition or because post-depositional processes have mixed grains of different depositional age. If the distribution can be attributed to partial bleaching, the minimum age model for determining D_e is appropriate. Before applying the model, a 20% σ_b value was added in quadrature to the error terms for each D_e value to account for expected intrinsic variation. The resulting minimum age D_e values are shown in Table 6. The distributions for each sample are displayed as radial graphs in Fig. 8.

Distinguishing partial bleaching from post-depositional mixing is not straightforward. The observation that some traps in quartz bleach quicker than others is often used to identify partial bleaching (e.g., Singarayer and Bailey, 2003). Linear-modulated OSL, where the power of the laser is steadily increased during read-out, often will provide a peak structure which makes it visually easier to distinguish fast and slow bleaching trap populations. LM-OSL was performed on 1500 grains (all 180–212 μm) from three samples (UW825-7). It was measured in this study after giving a dose upon completion of the SAR protocol. Ramping was from 0 to 90% power in 30 s. Only 62 grains provided a measurable signal. On 60 of these (97%), the LM-OSL curve was characterized by a sharp peak at the beginning of the ramp between 5 and 7% power, indicative of the presence of a fast-bleaching component. The other two had very low signals. Some curves are given in Fig. 7. On 77% of the grains the background was reached before 22% power. Of the 14 grains where a significant signal lingered beyond 22% — evidence of the presence of a slower component, — 8 were measured on grains where the natural D_e was determined and 6 were measured in the context of dose recovery. For the 8 where the natural D_e was determined, only one gave a D_e that was larger than the central age D_e of the entire sample. If grains with evidence of a slower component do not provide significantly "older" grains than the bulk, which is dominated by a fast component, there cannot be much evidence of partial bleaching. For the 6 measured in the context of dose recovery, five produced "D_e" values within 2σ of the administered dose, so there is no strong evidence slower components are causing signal build-up during the SAR sequence, which could result in younger ages.

Table 7
D_e value for each component as well as the proportion of grains assigned to each component.

Sample	Component 1		Component 2		Component 3	
	D_e (Gy)	%	D_e (Gy)	%	D_e (Gy)	%
UW823	4.2 ± 0.5	30.1	8.2 ± 0.5	69.9		
UW824	4.9 ± 0.3	77.7	9.8 ± 1.3	22.3		
UW825	1.9 ± 0.3	6.5	6.1 ± 0.3	73.5	12.9 ± 1.5	20.0
UW826	2.8 ± 0.5	26.6	4.9 ± 0.4	63.4	12.1 ± 1.4	10.0
UW827	1.4 ± 0.1	68.3	4.5 ± 0.3	31.7		

4.4. Ages

If the cause of high over-dispersion is neither dose rate heterogeneity nor partial bleaching, then post-depositional processes must be considered. It is not possible to choose the depositional age from the finite mixture model, even from the most common component, unless some understanding of the mixing process is available. If it can be assumed that grains moving up are more or less balanced by grains moving down, then the central age model might be appropriate, but otherwise other information is needed. For these samples, the D_e from the central age model is close to that of the most common component. The central age might be contrasted with the D_e from the minimum age model or from the lowest component. For either of the latter to be valid, one would have to assume some mixing process that brought older grains up but not younger grains down.

Table 8 gives the ages for each sample using both the central age and minimum age models and from the first two components of the finite mixture model. The most common component is in bold. In terms of stratigraphic expectations, UW823, UW824 and UW825 all relate to the lower lithic horizon, UW827 is younger than the upper lithic horizon, and UW826 lies between the two horizons. The age values are plotted with radiocarbon dates in Fig. 9. The central age and minimum age models produce dates that are in the correct stratigraphic order, within error terms. Neither the 1st or 2nd components do that. The most common component does but it does not distinguish between UW826 and the older samples nearly as well as either the central or minimum age models. This suggests the components are not describing discrete populations but rather continuous distributions that vary in their pattern from sample to sample, as the radial graphs show (Fig. 8). The central age dates are older than the radiocarbon dates and the minimum age dates are younger. Before offering an interpretation of these distributions, we first consider the lithic data.

5. Lithic technology, distribution and refitting

The central excavation area shows lithics concentrating in two modes. Fig. 10 gives the stratigraphic distribution of large lithic pieces (>2 cm) and smaller ones (<2 cm). Few large pieces are found in non-peak levels, but small pieces are scattered throughout, although still defining the same peaks. Almost half the small pieces come from between 190 and 220 cm depth. Another interesting feature is that for each peak the smaller pieces post-date the larger ones in one or two levels. This suggests smaller pieces are moving up.

Most small flakes between 190 and 220 cm are made of the highest quality raw material available in the region (fine-grained silicified sandstone and quartzite pebble cores, with occasional quartz and flint). They mainly relate to retouch and resharpening and are associated with final production stages of the formal bifacial and unifacial tools and the more sophisticated technology (Itaparica style) that predominates in the lower horizon (Bueno, 2005/2006, 2007a,b). In the upper horizon, stone quality is much more diverse and non-selective, with much less use of high quality material. Flaking on lower quality stone is more expedient with less standardized production sequences (Fig. 11). This relationship between macro- and micro- lithics supports the discreteness of the two occupations. Any post-depositional movement seems to involve mainly smaller flakes, and the direction seems to be movement up rather than movement down, because of the abrupt drop off in lithic concentration below 220 cm and because the fine-flaking materials associated with the lower horizon can be found scattered throughout the stratigraphy below 30–40 cm, but the lower quality material and expedient
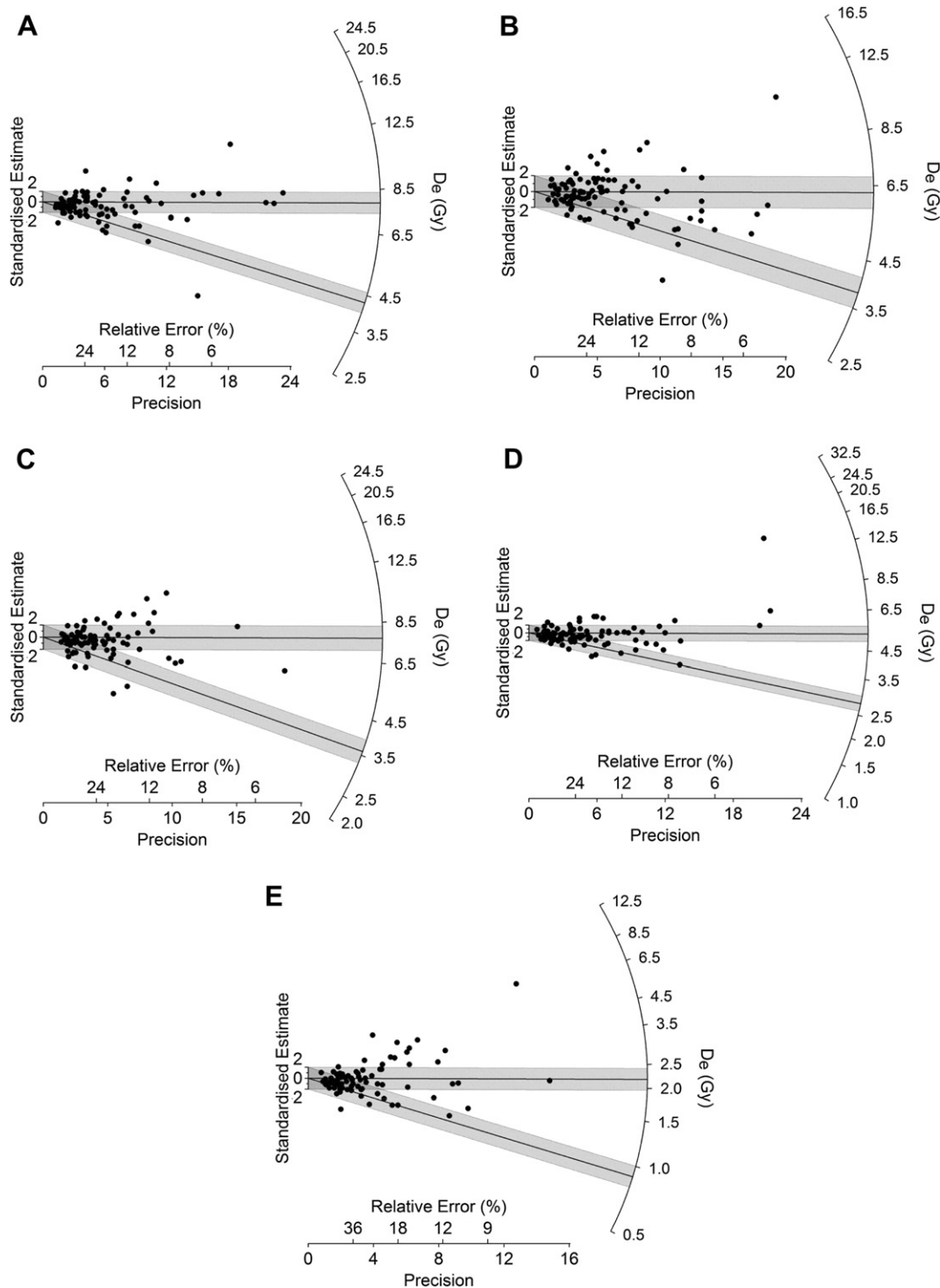
Fig. 8. Radial graph showing the distribution of equivalent dose values. Precision on the *x*-axis is plotted against a standardized D_e estimate for each value. The standardization is the difference between the measured D_e for a grain and some reference value, divided by the standard error on the D_e value for that grain. The shaded bands are centered on the D_e values determined by the central age model (upper) or minimum age model (lower), and they encompass all points consistent at two standard errors with these reference values. A line drawn from the origin on the standardized estimate axis through any point bisects the radial axis on the right at the D_e value for that point. A) UW823, B) UW824, C) UW825, D) UW826, E) UW827.

technology associated with the upper horizon are not often found below that horizon. Unique raw materials, which are easy to identify, reinforce this appearance of movement up. For example, in unit N1031/E1011, some retouching flakes of fine red silicified sandstone found about 80–100 cm are clearly associated with

a concentration of this material at 210 cm of the neighboring unit, N1032/E1011. Examples on other raw material types have also been noted. Some refitting also supports the integrity of the lower horizon, both within reduction sequences and among broken pieces. There are several examples that have been recorded, but

Table 8
Ages derived from the central age model, the minimum age model and the first two components of the finite mixture model. The component containing the most grains is in bold.

Sample	Age (ka) central age model	Age (ka) minimum age model	Age (ka) 1st component	Age (ka) 2nd component
UW823	13.3 ± 1.5	8.5 ± 1.2	8.4 ± 1.3	**16.3 ± 1.9**
UW824	13.5 ± 1.6	9.0 ± 1.1	**11.7 ± 1.4**	23.0 ± 4.0
UW825	13.7 ± 1.6	7.7 ± 1.1	4.1 ± 0.8	**13.0 ± 1.5**
UW826	9.7 ± 1.2	5.9 ± 1.0	6.1 ± 1.3	**10.4 ± 1.4**
UW827	4.2 ± 0.6	2.0 ± 0.4	**3.0 ± 0.4**	9.6 ± 1.3

no systematic study, which probably would have yielded many more, was done.

One further observation about the lithic assemblages from dune sites provides additional information about the sedimentary process at the site. None of the lithics, no matter from what depth, exhibit any patina. This is in contrast to other open air sites located outside the dune fields, on hardened older ground. It suggests rapid burial, which might also preserve the integrity of the horizons.

In sum, study of the lithics supports the discreteness of the horizons, although the distribution of tiny flakes does indicate some post-depositional upward movement of small (and light) material.

6. Dune formation processes and the archaeological record at Miracema

Analysis of lithic distribution seems to show that small flakes from the lower occupational level, representing curated technology, have moved considerably, mostly upward where they have
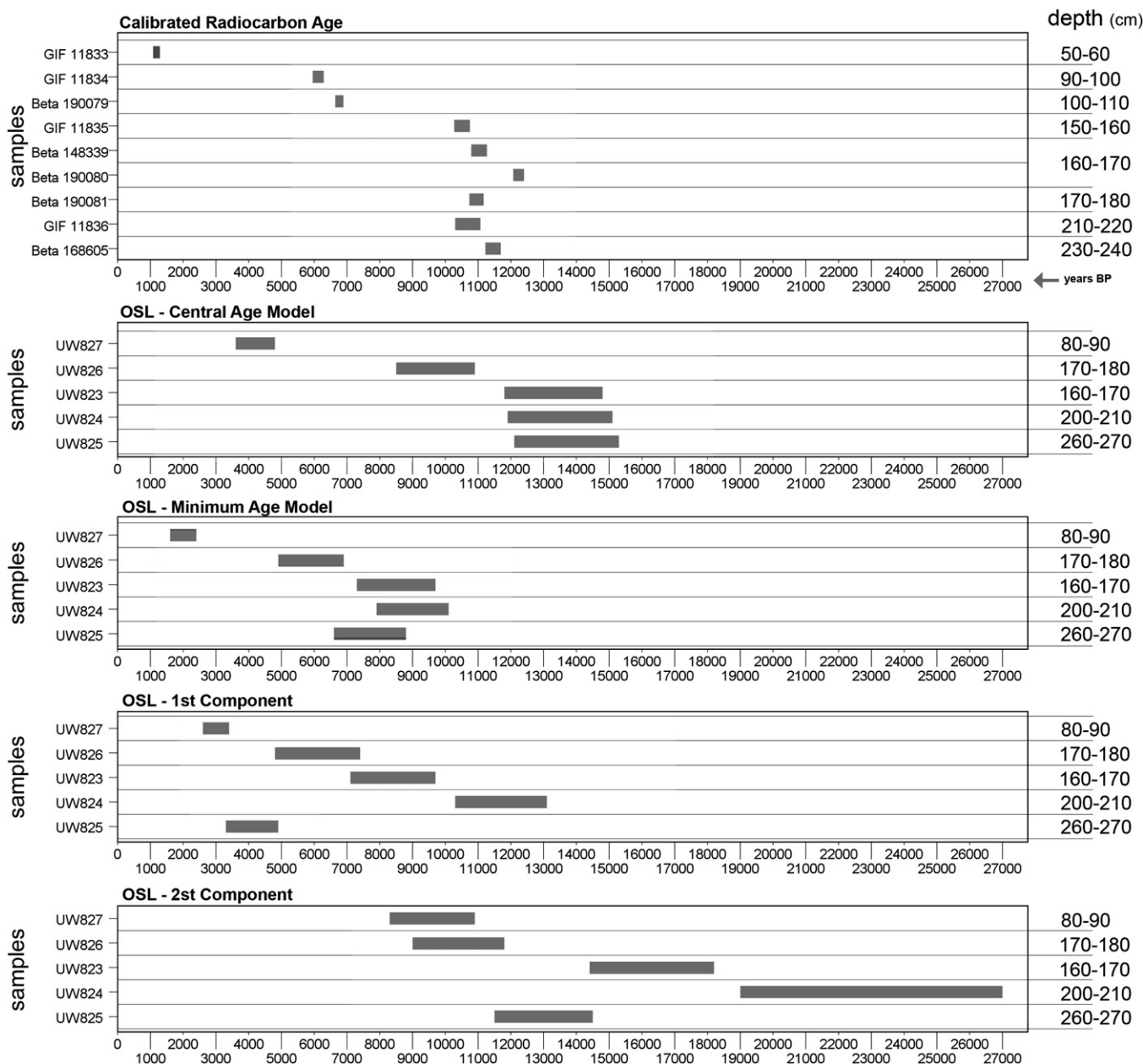
Fig. 9. Comparison of radiocarbon and luminescence dates, the latter using dates calculated from the central age model, the minimum age model and the first two components of the finite mixture model. Samples are listed in stratigraphic order rather than depth, because the samples came from different areas where stratigraphic changes occurred at different depths.
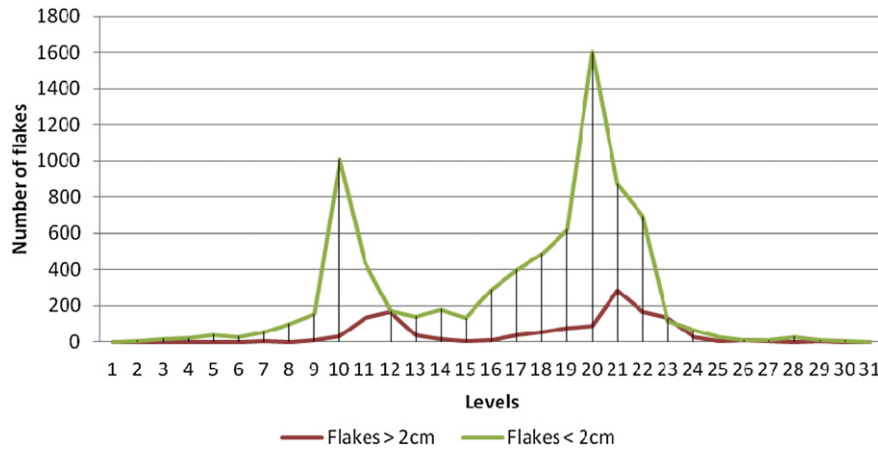
Fig. 10. Distribution of lithics of two size categories by excavation level.

become mixed with the more expedient technology of the upper occupation level. Quartz sand grains have also become mixed, according to the luminescence analysis. Quartz sand has likely migrated upward as well, but the mechanism is not clear. Excavations were not designed to deal with formation processes at this scale, so specific field data for evaluating the cause of this upward movement are lacking.

Fig. 11. Lithic data for each horizon from Miracema do Tocantins. A) Raw material distribution. B) Distribution of lithic remains. C) Flake type distribution.

Archaeological literature, although not concerned with movement of sand grains in particular, has considered the effect of post-depositional processes on the archaeological record (e.g., Cahen and Moeyersons, 1977; Wood and Johnson, 1978; Schiffer, 1987). In regards to unconsolidated sandy sediments, archaeologists have noted the fluidity of such deposits, by processes such as erosion, deflation, and pedoturbation, and how this has affected the content and spatial arrangement of artifacts (e.g., Moeyersons, 1978). But, "despite the implications of wind action on archaeological sites in an unconsolidated matrix, it appears that little research has been done on the subject" (Lancaster, 1986: p. 359). Most available studies are concerned with downslope (e.g., Rick, 1976) or downward (e.g., Courtin and Villa, 1982; Buck et al., 2002; Mayor, 2002) movements.

A few exceptions are worth mentioning in the context of the Miracema evidence. In an experimental study of lithic dispersion in an active dune environment, Lancaster (1986) found "stones of different morphology may be affected at different rates and different circumstances…smaller chips were found upwind and had further to go to leave the quadrat" (p. 362). One should have expected "more small stuff in the flaking areas than was evident from the size of the chips remaining and wind distribution tends to a more even distribution than originally has been deposited in desert areas." These comments are relevant to the Miracema evidence, which shows a more even distribution of small debitage than of larger, heavier items.

Rowlett and Robbins (1982) note that only about 10% of the materials move outside the original depositional area. The other 90% remain in the immediate vicinity. They further note, in similarity with Miracema, that only about 30% of the moving small materials descends. The rest ascends. Their figure (p78) shows a similar distribution as Fig. 10 in this paper.

The geological literature is also concerned with post-depositional change in sand dunes (e.g., Pye and Tsoar, 1990), but little information is available about movement of individual grains, largely because no tool, before single-grain luminescence analysis, has been available to assess it. Current discussion incorporates luminescence. Telfer (2011) studied the migration and reworking of longitudinal dunes in the Kalahari, using OSL dating in part to interpret his findings, although not at a single-grain level and only to show evidence of reworking, not individual grain movement. He suggests there are two modes of sediment deposition, one that results in dune progradation and one that simply reworks the upper most sands. Chronometric ages may reflect reworking, not original deposition. Others (e.g., Maxwell and Haynes, 2001) have also noted evidence of extensive reworking in upper layers and
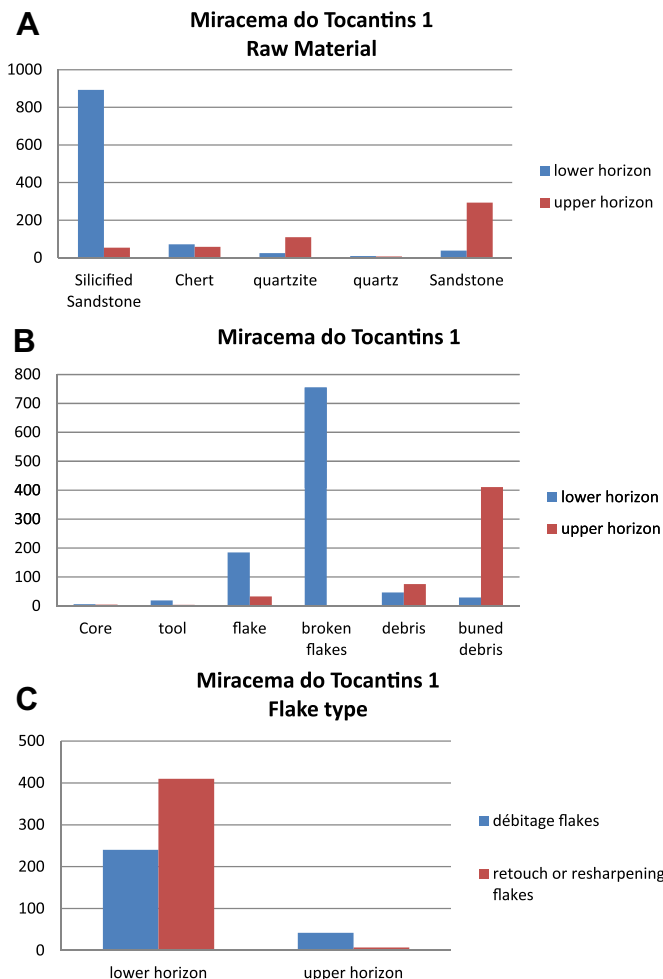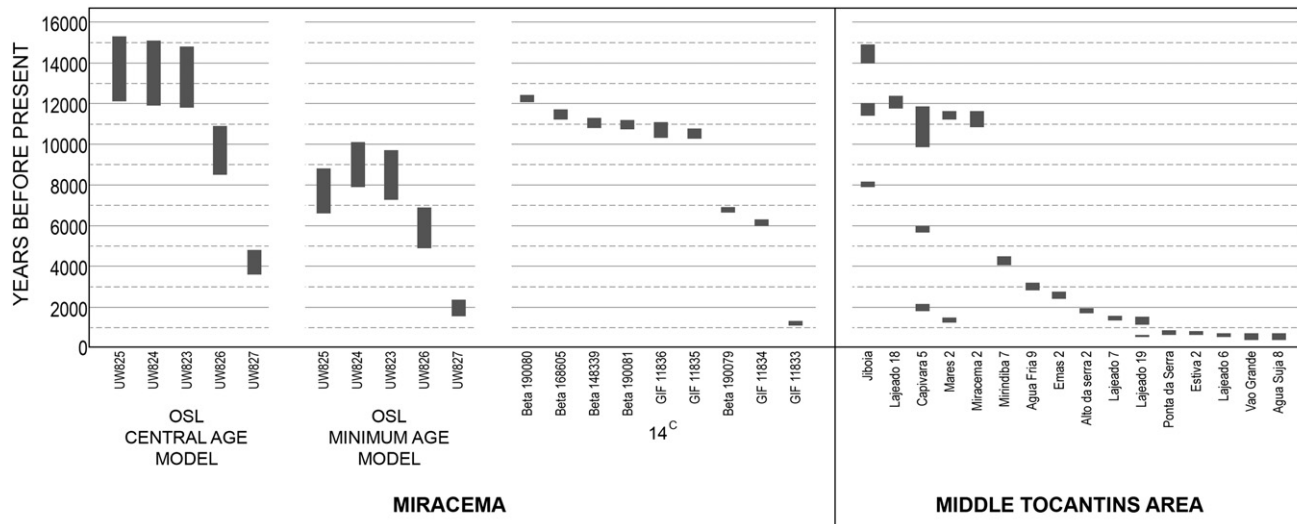
Fig. 12. Comparison of luminescence and radiocarbon dates from this paper with other dates from the literature (Bueno, 2008, 2007a,b). The other dates are all radiocarbon dates except for two luminescence dates on pottery for Lageado 19. The bars represent the calibrated range for radiocarbon and the 1-sigma confidence intervals for luminescence. Radiocarbon calibration is as in Table 2, except for Jiboia, which is calibrated with the INTCAL09 curve (Reimer et al., 2009).

varying loss of structure due to pedoturbation in lower layers. Roskin et al. (2011), in a chronological study of dunes in the Negev Desert, found that some of the OSL samples contained evidence of older grains, which apparently were due to reworking of older sediments without solar resetting. In another OSL dating study, Wright et al. (2011) argued that precise dates for aeolian activity are difficult to obtain "because sediments move and settle on various temporal scales of days, months or years (p: 14)."

Bateman et al. (2007) considered the effect of bioturbation on determining accurate depositional ages for aeolian sediments in four case studies from Florida and Texas. Both multi-grain and single-grain OSL were employed to complement independent age evidence from radiocarbon and artifact typology. They conclude that presence or lack of structure in the deposits is no indication of the extent of bioturbation, as their case studies show that lack of structure does not necessarily indicate bioturbation and that presence of structure does not necessarily preclude extensive bioturbation. They also showed that OSL dates in the correct stratigraphic order do not necessarily mean accurate depositional ages can be obtained. For a structureless deposit, such as that at Miracema, one case study showed extensive post-depositional particle movement, while another one showed some movement but not extensive. In the latter case, something similar to a minimum age model was employed to derive the depositional ages in order to exclude older grains that had moved upward.

The occupation levels at Miracema consist of several discrete clusters of lithic materials and charcoal arranged horizontally. The distribution of the small debitage laterally and upward from these clusters suggest post-depositional movement. The equivalent dose distributions also suggest post-depositional movement. Presumably sand grains would move up with the lithics, but is there movement in other directions and what are the mechanisms? The finite mixture analysis of equivalent dose, if translated into age, shows both younger and older components, neither of which provide correct stratigraphic order. Which if any of the components for any sample can represent the depositional age?

If sand particles have moved predominately upward, as the small lithics have, this might suggest that the minimum age model (unlike the youngest component which varies widely for every sample) may represent the depositional age, since older grains have been moved upward. Table 7 shows that for four of the five samples,

UW824 being the exception, the majority of the grains are much older than the minimum age, up to 90% for UW825. This would indicate extensive localized reworking. A possible mechanism is wind, the reworking by which is amply documented in the geological literature. But for this to explain the D_e distributions and the minimum age model as the appropriate model for depositional age, the extensive reworking would have to occur without exposing the sediment to light. Night wind is a possibility but hard to envision as the main reworking agent. Alternatively, maybe the minimum age model represents the age of reworking, not a depositional age. The depositional age then is older, but by how much? The central age model would make the depositional ages much older than the radiocarbon dates.

If not entirely wind, then bioturbation as a mechanism for reworking must be considered. There is no direct evidence of bioturbation, aside from some root extensions, but mixing evident in structureless sand bodies has been attributed to bioturbation in other places (e.g., Bateman et al., 2007).

A plausible explanation might be that both wind and bioturbation have reworked the Miracema deposits, exposing some grains to light but not all grains. Wind alone does not seem to account for all of the mixing because of the possibility of sunlight exposure, and the minimum age model may just represent those grains that were exposed. Wind, over a short distance, might also be expected to affect the sediments more or less uniformly, but the finite mixture model suggests more complicated structure. UW823, UW824 and UW825 should all be close to the same age, but the D_e distribution structure of UW825 differs significantly from the other two, while UW823 and UW824 differ substantially from each other in the proportional amount of grains in either component (Table 7, Fig. 8). Localized bioturbation therefore seems a likely compliment, moving grains but without necessarily any solar exposure.

If reworking has exposed some grains to light, then the minimum age model, as mentioned, will date the reworking, not the original deposition, and will therefore underestimate the age of occupation. The lithic data suggests that post-depositional movement has mainly been up, so sand grains have probably mainly moved up as well, including some without resetting. Any sample will thus have a component of older grains, not all of which may have been exposed. This would make the central age model an over-estimate. It is likely, therefore, that the true age of deposition will lie between

the ages from the minimum and central age models, which of course is where the radiocarbon dates fall. So while luminescence may not be able to produce precise dates for the deposition, it seems to support the reliability of the radiocarbon dates.

7. Conclusions

The stratigraphic distribution of lithic remains at Miracema do Tocantins shows two distinct cultural layers which are radiocarbon dated around 6–7 and 10.5–12.5 ka cal BP. Internal technological coherence and refitting provide confidence in the integrity of the two layers, but dispersion of small lithic debris throughout the stratigraphy as well as the OSL data suggest some post-depositional mixing. Larger lithic pieces do not appear to have moved significantly. The migration of lithic debris seems on technological grounds to be mainly upward. It is more difficult to understand the OSL D_e distributions, for while wind reworking may explain the movement of lithics, it does not seem likely, because of the probability of solar resetting, that this can explain fully the OSL distributions. Bioturbation seems a likely complementary mechanism. The depositional age likely falls between the ages estimated by the minimum age and central age models, which is where the radiocarbon dates lie. Understanding site formation processes is important for the interpretation of archaeological occupational contexts. OSL data, while not producing a precise age, have provided some understanding of the formation process, thus providing support for the cultural interpretation of the artifacts gained from lithic analysis and radiocarbon dating.

The composition and spatial distribution of the lithics indicate the site was formed by several short occupations generating several scatters of lithic remains along the flat dune tops. The lithic technology points to mainly resharpening activities on unifacial and bifacial tools produced elsewhere, probably nearer the river where pebble deposits and larger unstratified sites are found. Formal tools are intensely curated, which is characteristic of Itaparica sites.

Miracema do Tocantins is one among several other sites in a large hinterland riverine dune field, four others of which were partially excavated and have yielded radiocarbon dates of the same magnitude as at Miracema (Fig. 12). Miracema is among the first well described and dated open-air sites for the Pleistocene/Holocene transition in Central Brazil, thus a major contribution of this paper.

The spatial location of Miracema do Tocantins and its association with other nearby sites and natural resources (water, wood, lithic raw material) indicates that these sites are part of a wider area of exploration and circulation of mobile hunter-gatherer during the late Pleistocene/early Holocene. Certainly it involves the occupation of rock-shelters in the *serra* and open-air sites along the Tocantins river banks. On the basis of the technological sequences described and dated at Miracema, open-air sites can now be chronologically referenced and sorted for regional settlement approaches.

Most tested rockshelters in the area until now have not yielded evidence of human occupation for the same time frame detected at the dune sites. The only exception is the Jibóia rockshelter, located about 60 km south of the Miracema site, where testing has yielded two radiocarbon dates of around 12.5 and 7.5 ka cal BP. Unfortunately, insufficient material evidence prevents any consistent comparison. It makes clear, though, that ancient sheltered sites do exist in the Miracema/Lajeado area, with enormous potential for accessing Paleoindian settlement patterns and territoriality.

References

Ahlbrandt, T.S., Andrews, S., Gwynne, D.T., 1978. Bioturbation in eolian deposits. J. Sediment. Petrol. 48, 839–848.

Ab'Saber, A., 1982. Domínios morfoclimáticos atuais e Quaternários na região dos cerrados. Paleoclimas 10, 1–31.

Araujo, A., Neves, W. (Eds.), 2010. Lapa das Boleiras. Um sítio Paleoíndio do carste de Lagoa Santa, MG, Brasil. Annablume, São Paulo, p. 219.

Araujo, A.G.M., Feathers, J.K., Arroyo-Kalin, M., Tizuka, M.M., 2008. Lapa dos Boleiras rockshelter: Stratigraphy and formation processes at a paleoindian site in central Brazil. J. Archaeol. Sci. 35, 3186–3202.

Bateman, M.D., Boulter, C.H., Carr, A.S., Frederick, C.D., Peter, D., Wilder, M., 2007. Preserving the palaeoenvironmental record in drylands: bioturbation and its significance for luminescence-derived chronologies. Sediment. Geol. 195, 5–19.

Brady, N.C., 1974. The Nature and Properties of Soils. Macmillan, New York.

Buck, B.J., Kipp, J., Monger, H.C., 2002. Inverted clast stratigraphy in an eolian archaeological environment. Geoarchaeology 17, 665–687.

Bueno, L., 2005/2006. As indústrias líticas da região do Lajeado e sua inserção no contexto do Brasil Central. Rev. do Mus. de Arqueol. e Etnol. 15 (16) (São Paulo, Brasil).

Bueno, L., 2007a. Variabilidade tecnológica nos sítios líticos do Lajeado, TO. Rev. do Mus. de Arqueol. e Etnol. da USP (Suplemento 4), 215.

Bueno, L., 2007b. Organização tecnológica e teoria do design: entre estratégias e características de performance. In: Bueno, L., Isnardis, A. (Eds.), Das Pedras aos Homens. Tecnologia Lítica na Arqueologia Brasileira. Editora Argvmentvm, Belo Horizonte, pp. 67–94.

Bueno, L., 2008. The Early Holocene in Central Brazil: new dates from open-air sites. Curr. Res. Pleistocene 25, 29.

Bueno, L., 2011. L'occupation initiale du Brésil dans une perspective macro-régionale: les cas des régions de l'Amazonie, du Nordest et du Brésil. In: Vialou, D. (Ed.), Peuplements et Prehistoire de l'Amerique. Comitê de Travaux Historique et Scientifiques, Paris, pp. 209–220.

Cahen, D., Moeyersons, J., 1977. Subsurface movements of stone artefacts and their implications for the prehistory of Central Africa. Nature 266, 812–815.

Courtin, J., Villa, P., 1982. Une experience de piétinement. Bull. de la Soc. Préhist. Fran. 79 (4), 116–123.

Dias, A.S., 2004. Diversificar para poblar: El context arqueológico brasileño em La transición Pleistoceno-Holoceno, vol. 15. Complutum, Madri, Espanha, 249–263 pp.

Feathers, J.K., Piló, L., Arroyo-Kalin, M., Kipnes, R., Coblenz, D., 2010. How old is Luzia? Luminescence dating and stratigraphic integrity at Lapa Vermelha, Lagoa Santa, Brazil. Geoarchaeology 25, 395–436.

Feathers, J.K., Tunnicliffe, J., 2011. Effect of single-grain versus multi-grain aliquots in determining age for K-feldspars from southwestern British Columbia. Anc. TL 29, 53–58.

Fogaça, E., 2001. Mãos para o Pensamento. A variabilidade tecnológica de indústrias líticas de caçadores-coletores holocênicos a partir de um estudo de caso: as camadas VIII e VII da Lapa do Boquete (Minas Gerais, Brasil – 12.000/10.500 B.P.). Tese de Doutoramento apresentada ao Programa de Pós-Graduação em História, área de concentração: Arqueologia. Pontifícia Universidade Católica do Rio Grande do Sul, Faculdade de Filosofia e Ciências Humanas. Unpublished Dissertation.

Galbraith, R.F., Roberts, R.G., Laslett, G.M., Yoshida, H., Olley, J.M., 1999. Optical dating of single and multiple grains of quartz from Jinmium rock shelter, northern Australia: part I, experimental design and statistical models. Archaeometry 41, 339–364.

Guidon, N., 1986. A seqüência cultural da área de São Raimundo Nonato, Piauí, vol. 8. Clio, Recife, Brasil, 137–144 pp.

Kipnis, R., 1998. Early hunther-gatherers in the Americas: perspectives from central Brazil. Antiq 72, 581–592.

Kipnis, R., 2003. Long-term land tenure systems in Central Brazil. Evolutionary ecologya, risk management and social geography. In: Fitzhugh, B., Habu, J. (Eds.), Beyond Foraging and Collecting. Evolutionary Change in Hunterh-Gatherer Settlement Systems. Klwer Academic/Plenum Publishers, New York, pp. 181–230.

Lancaster, J., 1986. Wind action on stone artifacts: an experiment in site modification. J. Field Archaeol. 13, 359–363.

Ledru, M.-P., 1993. Late Quaternary environmental and climatic changes in central Brazil. Quaternary Res. 39, 90–98.

Leigh, D.S., 2001. Buried artifacts in sandy soils. In: Goldberg, P., Holliday, V.T., Ferring, C.R. (Eds.), Earth Sciences and Archaeology. Kluwer Academic/Plenum, New York, pp. 269–292.

Lourdeau, A., 2010. Le Technocomplexe Itaparica. Thèse Doctorat, Paris Ouest Naterre La Defense, 477 p.

Maxwell, T.A., Haynes, C.V., 2001. Sand sheet dynamics and Quaternary landscape evolution of the Selima Sand Sheet, southern Egypt. Quaternary Sci. Rev. 20, 1623–1647.

Mayor, J.H., 2002. Evaluating natural site formation processes in Aeolian dune sands: a case study from the Kmpotich Folsom site, Killpecker Dunes Wyoming. J. Archaeol. Sci. 29, 1199–1211.

Mayya, Y.S., Morthekai, P., Murari, M.K., Singhvi, A.K., 2006. Towards quantifying beta microdosimetric effects in single-grain quartz dose distribution. Radiat. Meas. 41, 1032–1039.

McCormac, F.G., Hogg, A.G., Blackwell Paul, G., Buck Caitlin, E., Higham, T.F.G., Reimer Paula, J., 2004. SHCal04 Southern Hemisphere calibration, 0–11.0 cal kyr BP. Radiocarbon 46 (3), 1087–1092.

Moeyersons, J., 1978. The behavior of stones and stone implements buried in consolidating and creeping Kalahari Sands. Earth Surf. Process. 3, 115–128.

Murray, A.S., Wintle, A.G., 2000. Luminescence dating of quartz using an improved single-aliquot regenerative-dose protocol. Radiat. Meas. 32, 57–73.

Oliveira, P., Marquis, R., 2002. Cerrados of Brazil. Columbia University Press, New York.

Oliveira, J. e., Viana, S., 1999/2000. O centro-oeste antes de Cabral. Rev. da USP 44, 142–187.

Prescott, J.R., Hutton, J.T., 1988. Cosmic ray and gamma ray dose dosimetry for TL and ESR. Nucl. Tracks Radiat. Meas. 14, 223–235.

Prous, A., Fogaça, E., 1999. Archaeology of the pleistocene–holocene boundary in Brazil. Quaternary Int. 53/54, 21–44.

Prous, A., Fogaça, E., e Ribeiro, L., 1998. Patrimônio Arqueológico. APA de Lagoa Santa – MG. IBAMA/CPRM, Belo Horizonte, 1–23 pp.

Prous, A., Rodet, J. (Eds.), 2009. Arqueologia do vale do rio Peruaçu e adjacências, vol. XIX. Arquivos do Museu de História Natural, Minas Gerais.

Pye, K., Tsoar, H., 1990. Aeolian Sand and Sand Dunes. Unwin Hyman, London.

Reimer, P.J., Baillie, M.G.L., Bard, E., Bayliss, A., Beck, J.W., Blackwell, P.G., Bronk Ramsey, C., Buck, C.E., Burr, G.S., Edwards, R.L., Friedrich, M., Grootes, P.M., Guilderson, T.P., Hajdas, I., Heaton, T.J., Hogg, A.G., Hughen, K.A., Kaiser, K.F., Kromer, B., McCormac, F.G., Manning, S.W., Reimer, R.W., Richards, D.A., Southon, J.R., Talamo, S., Turney, C.S.M., van der Plicht, J., Weyhenmeyer, C.E., 2009. IntCal09 and Marine09 radiocarbon age calibration curves, 0–50,000 Years cal BP. Radiocarbon 51 (4), 1111–1150.

Rick, J.W., 1976. Downslope movement and archaeological intrasite special analysis. Amer. Antiq 41, 133–144.

Roberts, R.G., Galbraith, R.F., Yoshida, H., Laslett, G.M., Olley, J.M., 2000. Distinguishing dose populations in sediment mixtures: a test of single-grain optical dating procedures using mixtures of laboratory-dosed quartz. Radiat. Meas. 32, 459–465.

Rodet, M.J., 2006. Etude Technologique des Industries Lithiques Taillées du Nord de Minas Gerais, Brésil - Depuis le Passage Pléistocène/Holocène jusqu'au Contact – XVIIIème Siècle. Thèse de Doctorat d'université de Paris X, Nanterre, 516 p. Unpublished Dissertation.

Rosa, A., 2004. Assentamentos pré-históricos da região de Serranópolis: análises de restos faunísticos. In: Schmitz, P., Rosa, A., Bittencourt, A. (Eds.), Arqueologia nos cerrados do Brasil Central. Serranópolis III. Pesquisas. Antropologia, vol. 60, pp. 221–264.

Roskin, J., Porat, N., Tsoar, H., Blumberg, D.G., Zander, A.M., 2011. Age, origin and climatic controls on vegetated linear dunes in the northwestern Negev Desert (Israel). Quaternary Sci. Rev. 30, 1649–1674.

Rowlett, R.M., Robbins, M.C., 1982. Estimating original assemblage content to adjust for post-depositional vertical artifact movement. World Archaeol. 14, 73–83.

Schiffer, M.B., 1987. Formation Processes of the Archaeological Record. University of New Mexico Press, Albuquerque.

Schmitz, P., 1980. A Evolução da cultura no sudoeste de Goiás. Pesquisas. série Antropologia 31, 41–84.

Schmitz, P., 1981. O Paleo-Índio, Anuário de Divulgação Científica de Goiás, 1–33 pp.

Schmitz, P., 1987. Prehistoric Hunters-gatherers of Brazil. J. World Prehist. 1, 53–125.

Schmitz, P.I., Rosa, A.O., Bittencourt, A.L., 2004. Arqueologia nos cerrados do Brasil do Brasil central. In: Serranópolis. Pesquisas, vol. 44.

Singarayer, J.S., Bailey, R.M., 2003. Further investigations of the quartz OSL components using linear modulation. Radiat. Meas. 37, 451–458.

Stuiver, M., Reimer, P.J., 1993. Extended 14C data base and revised CALIB 3.0 14C age calibration program. Radiocarbon 35 (1), 215–230.

Telfer, M.W., 2011. Growth by extension, and reworking, of a south-western Kalahari linear dune. Earth Surf. Process. Landforms 36, 1125–1135.

Wood, W.R., Johnson, D.L., 1978. A survey of disturbance processes in archaeological site formation. Adv. Archaeol. Meth. Theory, 315–381.

Wright, D.K., Forman, S.L., Waters, M.R., Ravesloot, J.C., 2011. Holocene eolian activation as a proxy for broad-scale landscape change on the Gila River Indian Community, Arizona. Quaternary Res. 76, 10–21.